ISSN 0021-3640, JETP Letters, 2020, Vol. 112, No. 4, pp. 257–261. © Pleiades Publishing, Inc., 2020.
Published in Russian in Pis'ma v Zhurnal Eksperimental'noi i Teoreticheskoi Fiziki, 2020, Vol. 112, No. 4, pp. 275–280.

CONDENSED MATTER

"Wetting" Phase Transitions by the Second Solid Phase for Linear Defects (Grain Boundary Triple Junctions)

A. B. Straumal[a, b], I. A. Mazilkin[a, b], K. V. Tsoi[a], B. Baretzky[c], and B. B. Straumal[a, b, c, *]

[a] *Institute of Solid State Physics, Russian Academy of Sciences, Chernogolovka, Moscow region, 142432 Russia*
[b] *National University of Science and Technology MISiS, Moscow, 119049 Russia*
[c] *Institute of Nanotechnology, Karlsruhe Institute of Technology, Eggenstein-Leopoldshafen, 76344 Germany*
**e-mail: straumal@issp.ac.ru*

Received July 16, 2020; revised July 21, 2020; accepted July 21, 2020

In this work, the wetting phase transition of grain boundaries (GBs) and their triple junctions (GB TJs) by the second solid phase in the magnesium-based alloy EZ33A is studied. The condition for complete wetting for the GB TJ ($\sigma_{GB} > \sqrt{3}\sigma_{SS}$) is weaker than that for GBs ($\sigma_{GB} > 2\sigma_{SS}$). Therefore, if the transition from partial to complete wetting occurs with increasing temperature, then all GB TJs should become completely wetted at a temperature T_{wTJ}, which is lower than the temperature T_{wGB}, at which all GBs become completely wetted. For the first time, it has been found experimentally that GB TJs are completely wetted at $T_{wTJ} = (380 \pm 10)$°C, which is approximately 70°C lower than $T_{wGB} = (450 \pm 10)$°C. The wetting phase at the GBs is the intermetallic compound $(Mg, Zn)_{12}RE$. A similar phenomenon was previously observed for GB TJ wetting with a liquid phase [B.B. Straumal, O. Kogtenkova, and P. Zieba, Acta Mater. **56**, 925 (2008)].

DOI: 10.1134/S0021364020160031

Phase transformations in solids is the instrument that allows one to control the structure of materials and purposefully change their properties. The phase transformations that are most frequently used by materials scientists when developing new and improving known materials include melting and solidification, formation and decomposition of a solid solution, amorphization, ordering and disordering, eutectic, peritectic, eutectoid and peritectoid transformations, allotropic phase transitions (for example, in iron, titanium, manganese, zirconium, etc.). However, in addition to such transformations that are observed in the bulk (or three-dimensional) phases, there are also phase transformations at interfaces (like grain boundaries and interphase boundaries). First of all, they include wetting phase transitions. The melt can completely or partially wet the grain boundaries (GBs). In the first case, the melt layer completely separates one grain from another and the contact angle between the liquid and solid phases is zero. In the second case, the melt does not completely cover the interface, the liquid phase has the form of separate drops, and the contact angle along the line of contact between the interface and the liquid is not zero [1–4].

The transition from complete to incomplete wetting and vice versa can occur when the temperature or pressure changes [5–8]. Cahn, as well as Ebner and Saam, showed that wetting transitions at external surfaces or interfaces are true two-dimensional phase transformations [9, 10]. They can be of either first or second order (continuous) [11, 12]. As a result of the studies of GB wetting phase transitions, the new lines of these transformations are increasingly enriching the traditional bulk phase diagrams for three-dimensional systems [1–8, 11–14]. Therefore, for example, in two-phase regions of volume phase diagrams, where solid solution and melt are in equilibrium, the tie-lines of GB wetting phase transitions appear. Usually, these are two horizontal tie-lines limiting the temperature range in which GBs with different energies σ_{GB} become completely wetted one after another [1, 15, 16]. The lower of these tie-lines corresponds to the minimum wetting temperature $T_{w\,min}$ for the GBs with the highest energy $\sigma_{GB\,max}$. The upper tie-line corresponds to the maximum wetting temperature $T_{w\,max}$ for the GBs with the lowest energy $\sigma_{GB\,min}$. In GBs not only thick layers of a "true" bulk liquid phase can form, but also thin layers of specific GB phases. For example, the lines of prewetting and premelting GB phase transitions begin in the ends of wetting phase transitions tie-lines in S + L regions of a bulk phase diagram. They continue then into the single-phase region of a solid solution [2–6].

In addition to three-dimensional (bulk) phases and two-dimensional GBs, there are also one-dimensional (linear) defects in solids. Except the well-known dislocations, these also include the lines of the GB triple

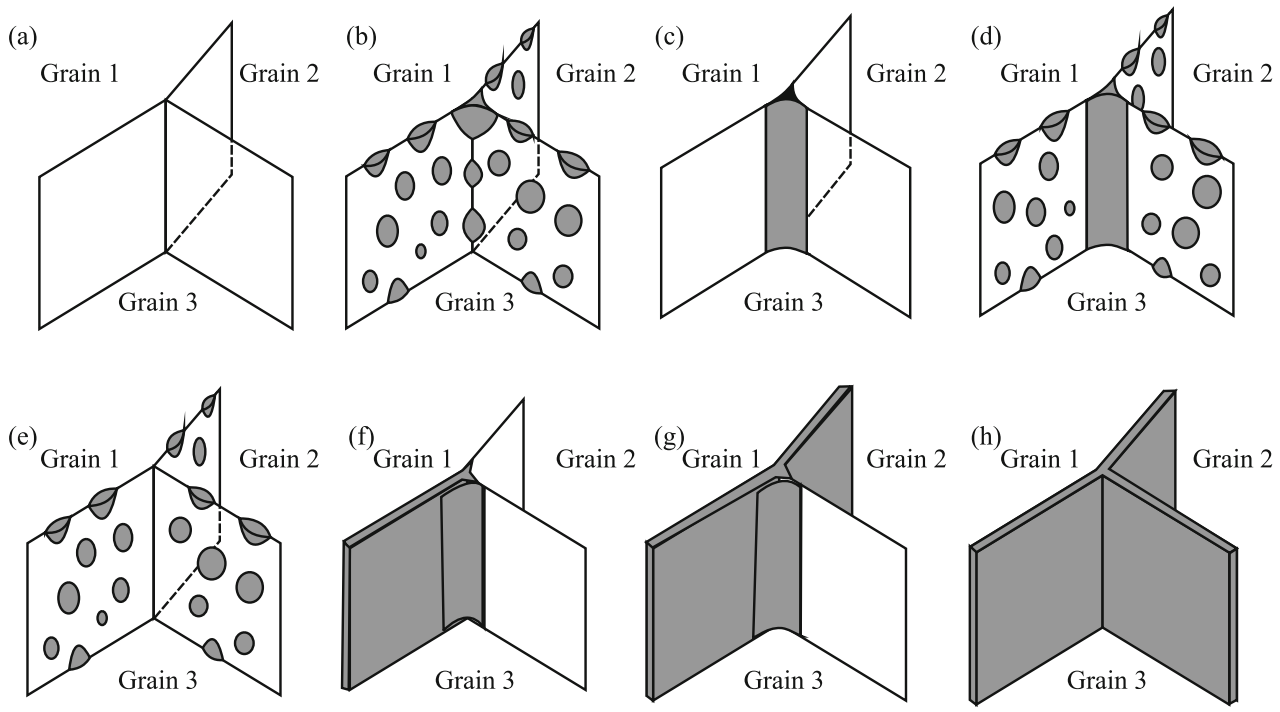

Fig. 1. Triple junction of GBs between grains 1, 2, and 3. (a) Dry TJ in contact with three dry GBs. (b) A partially wetted TJ in contact with three partially wetted GBs. (c) Fully wetted GB TJ in contact with three dry GBs. (d) Fully wetted TJ in contact with three partially wetted GBs. (e) A dry GB TJ in contact with three partially wetted GBs. (f) Completely wetted GB TJ in contact with one completely wetted GB. (g) Completely wetted GB TJ in contact with two completely wetted GBs. (h) Completely wetted GB TJ in contact with three completely wetted GBs.

junctions (GB TJs). It turns out that wetting phase transformations can also be observed in one-dimensional (linear) defects such as GB TJs or dislocations [17]. In the case of complete wetting, the linear defect is replaced by a liquid tube along its entire length. In the case of incomplete (partial) wetting, the chains of particles of the second phase are observed on the dislocation "decorating" them like beads [18]. The various possible combinations of completely and partially wetted GBs and TJs are shown schematically in Fig. 1. The wetting phase transformations of one-dimensional (linear) defects are even more difficult to observe than GB wetting ones. In the case of GB triple joints, the morphology of the wetting phase, in contrast to a dislocation, is more similar not to a tube, but to a trihedral prism, at the vertices of which there are the GBs.

The second phase, wetting GBs or triple joints, can be not only liquid but also solid [19–21]. The phenomena associated with the "wetting" of the GB by the second solid phase were observed in various systems: aluminum alloys [22], titanium alloys [23], tungsten alloys [24], steels [25], nickel-based superalloys [26], multicomponent alloys without the main component (so-called high-entropy ones) [27, 28], composites [29], welded and brazed joints [30].

Already D. McLean mentioned that the wetting of triple joints should occur under softer conditions than at the GBs [31]. Referring to the older work of Smith [32], McLean showed by a very simple calculation that GBs are completely wetted if $\sigma_{GB} > 2\sigma_{SL}$, and GB TJs are wetted if $\sigma_{GB} > \sqrt{3}\sigma_{SL}$ (here, σ_{SL} is the energy of solid–liquid interfaces). This fact logically leads to the difference in the temperatures T_w of the wetting transition for the GBs and GB TJs. It was shown [17] that the transition from partial to complete wetting of GB TJs occurs at a temperature T_{wTJ}, which is lower than that for GB wetting transition T_{wGB}. However, the question about the ratio of the wetting transition temperature for the GBs T_{wGB} and GB TJs T_{wTJ} in case of the wetting by a second solid phase, remains open. This work should answer this question.

The wetting of GBs and their triple joints with the second solid phase was studied on polycrystals of magnesium-based alloy EZ33A (provided by CanMet Materials, Canada). The alloy contains (in mass percent) 2.5% Zn, 0.4% Zr, 3% rare earth elements (RE), the rest is magnesium. Rare earth metals were added during smelting to the Mg–Zn–Zr alloy in the form of "mischmetal," consisting mainly of cerium, lanthanum, and neodymium. The 2-mm-thick discs were cut from the cast ingot EZ33A using electric spark cut-

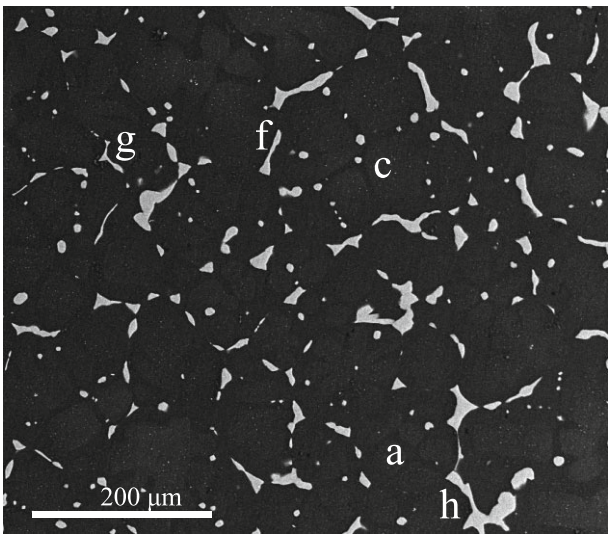

Fig. 2. Microstructure of the EZ33A alloy after annealing at 150°C, obtained by SEM (backscattered electrons). Magnesium-rich matrix looks dark; the wetting layers on the GBs and TJs look bright. Differently wetted GBs and TJs are marked with letters according to the diagram in Fig. 1.

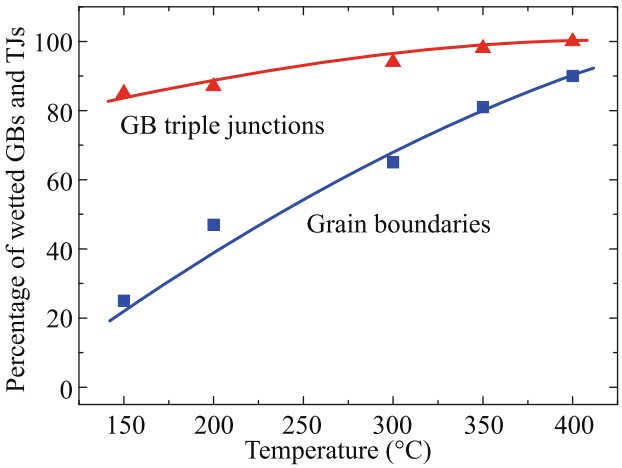

Fig. 3. (Color online) Temperature dependences of the portion of wetted GBs and triple joints. Upper curve (filled triangles) represents the sum of the wetted triple joint configurations shown in Figs. 1c, 1f–1h. Lower curve (filled squares): completely wetted GBs.

ting. The samples were chemically etched in a solution of 75% HCl + 25% H_2O. After cutting, the samples were placed in evacuated quartz ampoules (residual pressure 4×10^{-4} Pa) to prevent oxidation. Then the samples were annealed at 150°C, 1826 h; 200°C, 2371 h; 300°C, 100 h; 350°C, 100 h, and 400°C, 150 h. After quenching, the samples were embedded in an electrically conductive resin, mechanically ground, and polished. The polished samples were examined using a LEO 1530 VP scanning electron microscope (SEM) equipped with an EDX detector and a backscatter detector (EBSD).

A quantitative analysis of the wetting transition was performed using the following criterion: each GB was considered completely wetted only when the layer of the second solid phase completely covered the GB (all three GBs in Fig. 1h). If such a layer turned out to be interrupted, the GB was considered partially (incompletely) wetted (all three GBs in Figs. 1b, 1d, and 1e). If the second solid phase was absent in the GB, it was considered as "dry" (all three GBs in Fig. 1a). Likewise, a GB TJ was considered wet if a triangle of the second solid phase was visible in the TJ (Figs. 1c, 1d, 1f–1h), in other cases the junction was considered as dry (Figs. 1a, 1e). Careful sequential grinding of the annealed samples did not reveal any partially wetted TJ (shown in the diagram in Fig. 1b). Therefore, they were not considered in the analysis. Along with dry TJs, we counted separately wetted TJs in contact with three (Fig. 1h), two (Fig. 1g), one (Fig. 1f) or none (Fig. 1c) wetted GBs. At least 500 GBs and/or GB TJs were analyzed at each temperature.

Figure 2 shows a SEM micrograph of the structure of the EZ33A alloy after annealing at 150°C. Magnesium-rich matrix looks dark; the wetting layers of the second solid phase, rich in rare-earth metals, in GBs and TJs, look bright. The different types of wetted GBs and TJs are marked in Fig. 2 with letters corresponding to the diagram in Fig. 1. The wetting phase in the GBs is the intermetallic compound $(Mg, Zn)_{12}RE$ [33]. In the EZ33A alloy, the GB wetting by the melt was also observed (at higher temperatures) [34].

Figure 3 shows the temperature dependences of the portion of wetted GBs and TJs. The filled triangles (upper curve) represent the portion of wetted triple joints. It includes the sum of the configurations shown in Figs. 1c, 1f–1h. The portion of wetted GB TJs grows with increasing temperature: at 150°C, it is ~85%. At $T_{wTJ} = (380 \pm 10)$°C, all triple joints are already "wetted" by the second solid phase. The filled squares (bottom curve) show the portion of completely wetted GBs. It also grows with increasing temperature from ~25% at 150°C to ~90% at 400°C. Thus, the portion of fully wetted GBs is everywhere lower than the portion of wetted TJs. If we extrapolate the fraction of completely wetted GBs to 100%, then we can determine the temperature $T_{wGB} = (450 \pm 10)$°C. Thus, 100% wetting by the second solid phase of triple joints occurs (70 ± 10)°C earlier (i.e., at a lower temperature) than 100% wetting of all GBs.

Consider a GB in equilibrium contact with the second solid phase. The second solid phase can completely wet the GB if $\sigma_{GB} > 2\sigma_{SS}$. In other words, the GB energy σ_{GB} should be higher than the energy of two solid/solid interfaces $2\sigma_{SS}$ (see the diagram in Figs. 4a, 4b). In case of GB complete wetting, GB must be replaced with a layer of the second solid phase

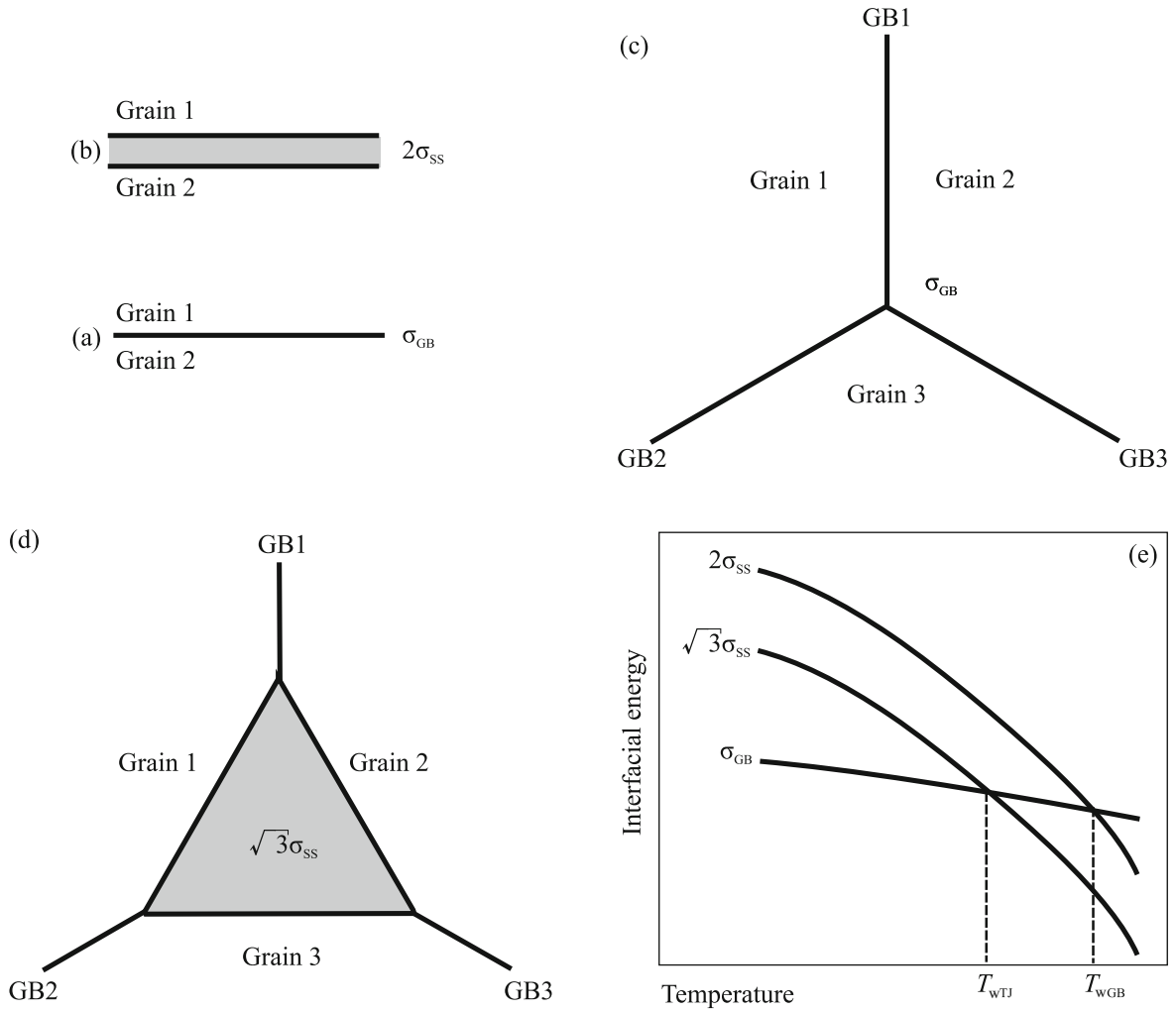

Fig. 4. (a) Dry GB with energy σ_{GB}. (b) Completely wetted GB, replaced by a layer of the second solid phase (shown in dark gray) and two interphase boundaries with an energy of $2\sigma_{SS}$. (c) Dry TJ with three boundaries having the same energy σ_{GB}. (d) Triple joint of the GBs, replaced by the triangle of the second solid phase (the case of complete wetting of the GB TJ). (e) Temperature dependence for the GB energy σ_{GB}, the energy of two interphase boundaries $2\sigma_{SS}$, as well as the energy of the interphase boundaries of two solid phases $\sqrt{3}\sigma_{SS}$ in a triangular prism surrounding a completely wetted GB TJ.

and two interphase boundaries "solid phase/solid phase" (Fig. 4b). Let us now consider a triple joint in the same alloy. The second solid phase can completely wet also GB TJ. In this case, a triangular prism filled with the second solid phase replaces the GB TJ (Figs. 4c, 4d). In this case, the "star" of three GBs (Fig. 4c) is replaced by a triangle of three interphase boundaries (Fig. 4d). In the simplest case of an ideal symmetric TJ with the same boundaries having the same σ_{GB}, the condition of complete wetting should be $\sigma_{GB} > \sqrt{3}\sigma_{SS}$. This condition is less strong that for GBs ($\sigma_{GB} > 2\sigma_{SS}$). Here we consider a wetted TJ of a macroscopic size (at least several microns) and, thus, in the first approximation, we neglect the energy σ_{TJ} of the TJ itself. Both σ_{GB} and σ_{SS} decrease with increasing temperature due to a decrease in elastic moduli (Fig. 4e). If the temperature dependences $\sigma_{GB}(T)$ and $\sigma_{SS}(T)$ intersect at T_{wGB} below the melt appearance temperature T_m, then at T_{wGB} a wetting phase transition occurs. Below T_{wGB}, GBs can coexist in equilibrium contact with the second solid phase. Above T_{wGB}, GBs must be replaced by a layer of the second solid phase. Thus, GB cannot coexist in equilibrium contact with the second solid phase and must disappear. The temperature dependence $\sqrt{3}\sigma_{SS}(T)$ lies below the dependence $2\sigma_{SS}(T)$ (Fig. 4e). Therefore, $\sqrt{3}\sigma_{SS}(T)$ intersects with $\sigma_{GB}(T)$ at a T_{wTJ} temperature, which is below T_{wGB}. As a result, completely wetted GBs are absent in the polycrystal in the temperature range between T_{wTJ} and T_{wGB}. However, completely

wetted TJs can exist in the temperature range between T_{wGB} and T_{wTJ}.

Thus, we observed in this work the transition from incomplete to complete wetting by the second solid phase for GBs and their triple joints with increasing temperature. In the studied magnesium alloy EZ33A, TJs, and GBs are wetted by the intermetallic compound $(Mg, Zn)_{12}RE$. It is shown experimentally that in this case all GB TJs become completely wetted at a temperature T_{wTJ}, which is lower than the T_{wGB} temperature, at which all GBs become completely wetted. The temperature T_{wTJ} was $T_{wTJ} = (380 \pm 10)°C$. This value is approximately 70°C lower than the temperature of complete wetting of all GBs $T_{wGB} = (450 \pm 10)°C$.

FUNDING

The work was supported by the Russian Science Foundation (project no. 18-72-00243).

REFERENCES

1. E. I. Rabkin, L. S. Shvindlerman, and B. B. Straumal, Int. J. Mod. Phys. B **5**, 2989 (1991).
2. L.-S. Chang, E. Rabkin, B. Straumal, P. Lejcek, S. Hofmann, and W. Gust, Scr. Mater. **37**, 729 (1997).
3. L.-S. Chang, E. Rabkin, B. B. Straumal, S. Hoffmann, B. Baretzky, and W. Gust, Def. Dif. Forum **156**, 135 (1998).
4. L.-S. Chang, B. B. Straumal, E. Rabkin, W. Gust, and F. Sommer, J. Phase Equilib. **18**, 128 (1997).
5. O. I. Noskovich, E. I. Rabkin, V. N. Semenov, B. B. Straumal, and L. S. Shvindlerman, Acta Metall. Mater. **39**, 3091 (1991).
6. B. B. Straumal, O. I. Noskovich, V. N. Semenov, L. S. Shvindlerman, W. Gust, and B. Predel, Acta Metall. Mater. **40**, 795 (1992).
7. B. B. Straumal, B. S. Bokstein, A. B. Straumal, and A. L. Petelin, JETP Lett. **88**, 537 (2008).
8. B. Straumal, E. Rabkin, W. Lojkowski, W. Gust, and L. S. Shvindlerman, Acta Mater. **45**, 1931 (1997).
9. J. W. Cahn, J. Chem. Phys. **66**, 3667 (1977).
10. C. Ebner and W. Saam, Phys. Rev. Lett. **38**, 1486 (1977).
11. B. B. Straumal, A. S. Gornakova, O. A. Kogtenkova, S. G. Protasova, V. G. Sursaeva, and B. Baretzky, Phys. Rev. B **78**, 054202 (2008).
12. B. B. Straumal, A. S. Gornakova, V. G. Sursaeva, and V. P. Yashnikov, Int. J. Mater. Res. **100**, 525 (2009).
13. B. B. Straumal and B. Baretzky, Interface Sci. **12**, 147 (2004).
14. O. A. Kogtenkova, B. B. Straumal, S. G. Protasova, A. S. Gornakova, P. Zięba, and T. Czeppe, JETP Lett. **96**, 380 (2012).
15. E. L. Maksimova, L. S. Shvindlerman, and B. B. Straumal, Acta Metall. **36**, 1573 (1988).
16. B. B. Straumal, P. V. Protsenko, A. B. Straumal, A. O. Rodin, Yu. O. Kucheev, A. M. Gusak, and V. A. Murashov, JETP Lett. **96**, 582 (2012).
17. B. B. Straumal, O. Kogtenkova, and P. Zięba, Acta Mater. **56**, 925 (2008).
18. S. Prokofjev and E. Johnson, J. Phys. Commun. **1**, 055001 (2017).
19. B. B. Straumal, O. A. Kogtenkova, A. B. Straumal, Yu. O. Kuchyeyev, and B. Baretzky, J. Mater. Sci. **45**, 4271 (2010).
20. B. B. Straumal, O. A. Kogtenkova, K. I. Kolesnikova, A. B. Straumal, M. F. Bulatov, and A. N. Nekrasov, JETP Lett. **100**, 535 (2014).
21. B. B. Straumal, O. A. Kogtenkova, A. B. Straumal, and B. Baretzky, Lett. Mater. **8**, 364 (2018).
22. A. Mochugovskiy, N. Tabachkova, and A. Mikhaylovskaya, Mater. Lett. **247**, 200 (2019).
23. V. N. Chuvil'deev, V. I. Kopylov, A. V. Nokhrin, P. V. Tryaev, N. Y. Tabachkova, M. K. Chegurov, N. A. Kozlova, A. S. Mikhaylov, A. V. Ershova, M. Y. Gryaznov, I. S. Shadrina, and C. V. Likhnitskii, J. Alloys Compd. **785**, 1233 (2019).
24. S. Tamang and S. Aravindan, Mater. Lett. **254**, 145 (2019).
25. Y. Luo, H. Guo, X. Sun, M. Mao, and J. Guo, Metals **7**, 27 (2017).
26. M. Rafiei, H. Mirzadeh, and M. J. Sohrabi, Mater. Lett. **266**, 127481 (2020).
27. D. E. Jodi and N. Park, Mater. Lett. **256**, 126654 (2019).
28. D. E. Jodi, J. Park, and N. Park, Mater. Charact. **157**, 109888 (2019).
29. T. A. Krylova and Yu. A. Chumakov, Mater. Lett. **274**, 128022 (2020).
30. L. Maj and J. Morgiel, Mater. Lett. **189**, 38 (2017).
31. D. McLean, *Grain Boundaries in Metals* (Clarendon, Oxford, 1957), p. 95.
32. C. H. Smith, Trans. AIMME **175**, 15 (1948).
33. K. Bryla, J. Morgiel, M. Faryna, K. Edalati, and Z. Horita, Mater. Lett. **212**, 323 (2018).
34. A. B. Straumal, K. V. Tsoi, I. A. Mazilkin, A. N. Nekrasov, and K. Bryla, Arch. Metall. Mater. **64**, 869 (2019).